

LITERATURE REVIEW

2.1 Overview of dragline

The dragline is heavy-duty, cyclic equipment that moves broken rock material from one position to another while sitting at one position. The conventional role of dragline in an open cut strip coal mine is to uncover the mineral by removing the overburden rocks (figure 2.1). The dragline mining is a relatively simple, versatile, low- cost, mining method. A single dragline has the capability of operating over a wide range of overburden depths for the different material characteristic (Humphrey, 1990). Draglines are considered as “Kingpin” of any mining site because of its high capacity and capital cost (Sahu and Naik, 2015). These machines need to be operated in such a way that, the optimum return from the investment and desired coal production rate can be achieved.



Figure 2.1 Dragline in a coal mine (Anonymous, 2008)

Chapter 2: Literature Review

The first dragline was invented by John W. Page in 1904, the founding father of Page Company. The employer then merged with The Harnischfeger Corporation P&H, in 1988. Other two companies in dragline marketplace, Marion Steam Shovel Dredge and Bucyrus additionally merged under the name of Bucyrus. Today, Bucyrus and P&H are most popular dragline producer in the international market.

Use of dragline in the mining industry for the removal of the overburden in stripping enhances productivity by up to 40 per cent in comparison to the shovel-truck method (Ozdogan, 1984). The economic comparison of a truck shovel and a dragline has been shown in figure 2.2.

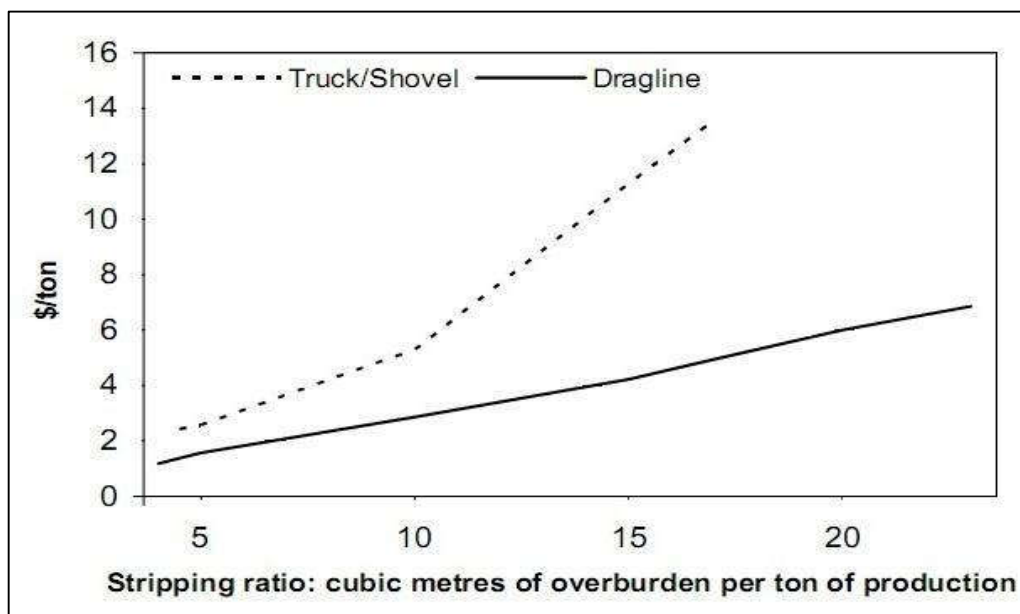


Figure 2.2 Economic comparison of a truck shovel and dragline (Hartman, 2002)

Different size and capacity dragline are used for different mining applications. There are many factors affecting the method of working with dragline, namely, geology, dragline characteristics, mine production targets, coal and overburden thickness, nature of formation, formation stability of the area, number of coal seams, design of

blasting, loose material strength and dragline line operator skills etc. (Mirabediny and Baafi, 1998).

Length of a dragline pit is tormented by the factors which include topographical and geological adjustments and human-based handicaps (Hartman, 1992). On the other hand, the width of the pit is consistent with, dragline specification inclusive of maneuverability, dumping radius, movement charge, and layout parameters (Hartman, 1992).

2.2 Dragline operations in India

Indian mineral industry has contributed significantly to make the nation self-sufficient in coal. To meet the increasing demands of thermal, cement and other users, the production of coal and lignite in their respective sectors have shown a significant increasing trend over last few years. While extracting the deep-seated coal deposit and also to increase the present production capacity, the coal mines have been compelled to modernize the mining technology, particularly in the fields of blasting. Coal producers have already tried to open up big surface coal mines in various coalfields. This has further imposed the importance of adopting better mining technology in the above mines by applying systematic and cost-effective approaches while selecting the mining equipment and introducing the state-of-the-art technology. In India, the development of giant surface mining ventures like Bina and Jayant with setting up of higher coal production targets (up to 10 million tonnes per annum) calls for systems to remove large volume of overburden in shortest possible time. This has resulted in major changes in overburden/ interburden excavation technology in

surface coal mines from shovel mining to that of draglines. The dragline currently used in India is tabulated in table 2.1 with their specifications and their locations.

Table 2.1: List of dragline used in Indian coal mines. (Patel R.K. et. al., 2017)

Company	Project	Dragline Specification	Numbers
BCCL (CIL)	Block II	24/96	1
BCCL(CIL)	Joyrampur	5/45	1
ECL(CIL)	Sonepur Bazari	26/82	1
MCL(CIL)	Balanda	4/45,10/60, 11.5, 20/90	4
MCL(CIL)	Belpahar	10/70	1
MCL(CIL)	Lajkura	10/70	1
MCL(CIL)	Samalleshwari	10/70	1
NCL(CIL)	Amlori	24/96	3
NCL(CIL)	Bina	10/70-2 nos., 24/96- 2 nos	4
NCL(CIL)	Dudhichua	24/96 – 4 nos.	4
NCL(CIL)	Jayant	15/90 -1 no., 24/96 -3 nos.	4
NCL(CIL)	Khadia	20/90 – 2 nos.	2
NCL(CIL)	Nigahi	20/90 – 2 nos., 24/96 – 2 nos.	4
NCL(CIL)	Krishnashila	33/70	1
SECL (CIL)	Bisrampur	30/76 – 2 nos.	2
SECL(CIL)	Chirimiri	10/70	1
SECL (CIL)	Dhanpuri	10/70 -1no., 20/90 -1 no.	2
SECL(CIL)	Dola/Rajnagar	10/70	1
SECL (CIL)	Jamuna	5/45 -1 no. , 10/70 – 1 no.	2
SECL(CIL)	Kurasia	5/45 -1no.,10/70 -1no., 11.5 -1no	3
WCL(CIL)	Ghughus	24/96	1
WCL(CIL)	Sasti	20/90	1
WCL(CIL)	Umrer	4/45 -1no., 7cum-1no., 15/90 -1 no.	3
SASAN (RELIANCE)	Singrauli	62/100	2

2.3 Dragline Selection

While incorporating a new dragline, the selection process is based on optimum dragline dimensions required for the excavation and spoiling operations and the production requirements of the selected mine. The primarily considered parameters for selection of the machine are as follows (Sweigard, 1992)

1. Dragline reach
2. Maximum dig depth
3. Maximum dump height
4. Bucket capacity.

Along with the above listed parameters, the speed specifications of the equipment such as swing speed, hoist and payload speed also be considered. After selection of these parameters, sufficient dragline models, which come across these criteria, can be chosen. If there are several dragline options which fulfill the above parameters, there are a lot of other factors that may affect the selection process. In determining these factors, range diagrams, graphs and tables, and computations can be utilized.

2.3.1 Reach factor of the dragline

Reach factor is one of the most significant parameters in selection of the dragline equipment. Reach factor is total of the distance that dragline machine have to reach on both dragging and dumping operations (figure 2.3). The computation can be carried out using equation 2.1 and 2.2.

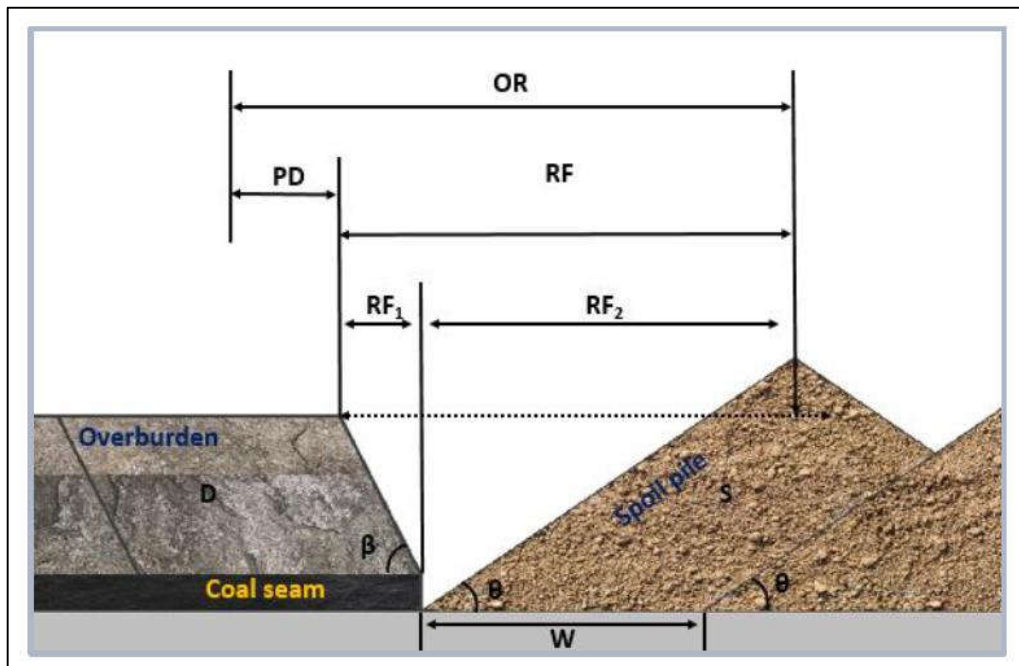


Figure 2.3 Reach Factor and operation radius

$$RF = RF1 + RF2 = \frac{D}{\tan\beta} + \frac{H}{\tan\theta} \quad (2.1)$$

$$RF = \frac{D}{\tan\beta} + \frac{D \times SF}{\tan\theta} + \frac{W}{4} \quad (2.2)$$

Where

RF1 Reach distance required to reach spoiling area (m)

RF2 Reach distance along the spoil pile to the dumping point (m)

θ Spoil pile angle (degree)

β Pit slope angle (degree)

SF Swell factor of broken overburden material according to blasting conditions

D Overburden thickness (m)

W Pit width (m)

H Spoil pile height (m)

2.3.2 Bucket Capacity

Bucket capacity is the capacity of the bucket required to handle the task. The bucket capacity requirement increases by increasing swell factor condition and decreases with the high operating time, dragline availability and dragline utilization and the operation cycle time. Also higher the fill ability of bucket lowers the required capacity the bucket (Karpuz and Demirel, 2016). The required bucket capacity is computed by using equation 2.3 and 2.4.

$$BC = \frac{OB_T \times SF \times CT}{O \times A \times U \times BF} \quad (2.3)$$

$$BC = \frac{OB_T \times SF \times CT}{OP \times BF} \quad (2.4)$$

Where:

BC: Required bucket capacity (m³)

CT: One cycle time of dragline (hr.)

BF: Bucket fill factor

OP: Total operation time of dragline (hr/yr)

U: Dragline utilization factor

A: Dragline availability factor

O: Dragline operating time (hr/yr)

SF: Swell factor of broken overburden material according to blasting conditions.

OB_r: Total overburden removed per year (m³/year)

2.3.3 Maximum Suspended Load (MSL)

This parameter is used to assess the allowable (maximum) suspended load of equipment's from chart or catalogues. Equation 2.5 reveals that MSL is the sum of the dead weight W_D and pay load W_L of loaded bucket that can dragline lift (Karpuz and Demirel, 2016).

$$MSL = W_D + W_L \quad (2.5)$$

Where:

MSL: Maximum suspended load (kg)

W_D: Dead weight of bucket (kg)

W_L: Pay load of bucket (kg)

After calculating reach factor and bucket capacity required the dragline can be chosen based on the chart provided by various dragline manufacturers for the value of maximum suspended load and reach factor combination.

2.3.4 Selection Chart

Selection of the dragline with the help of charts is much easier and faster. However, this selection process is not much accurate and also it is very tough to add new models in to the chart. Selection chart is basically a two dimensional (2-D) graph with maximum allowable load and reach factor parameters of models (figure 2.4). For selecting an optimum model after calculations of these parameters the nearest models to the crossing point of MSL and RF have to be considered for selection.

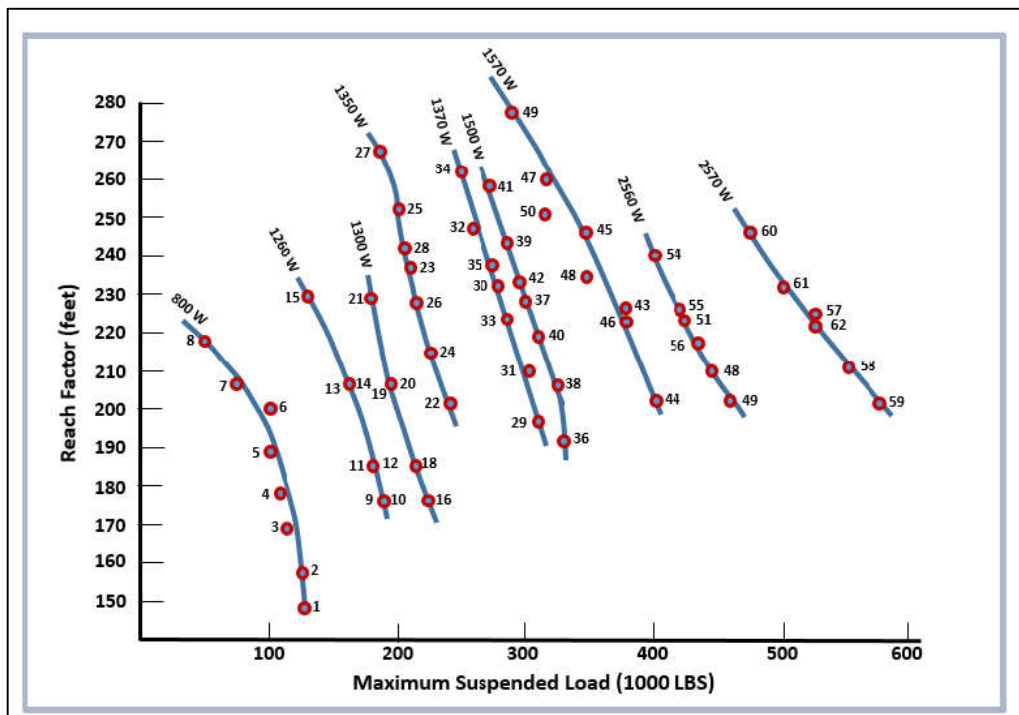


Figure 2.4 Dragline standard selection chart (Bucyrus Erie Company, 1977)

2.4 Assembly of Dragline

In a typical dragline design, a number of components are required for its construction. These components are assembled at the installation site. Basic components of dragline are shown in figure 2.5.

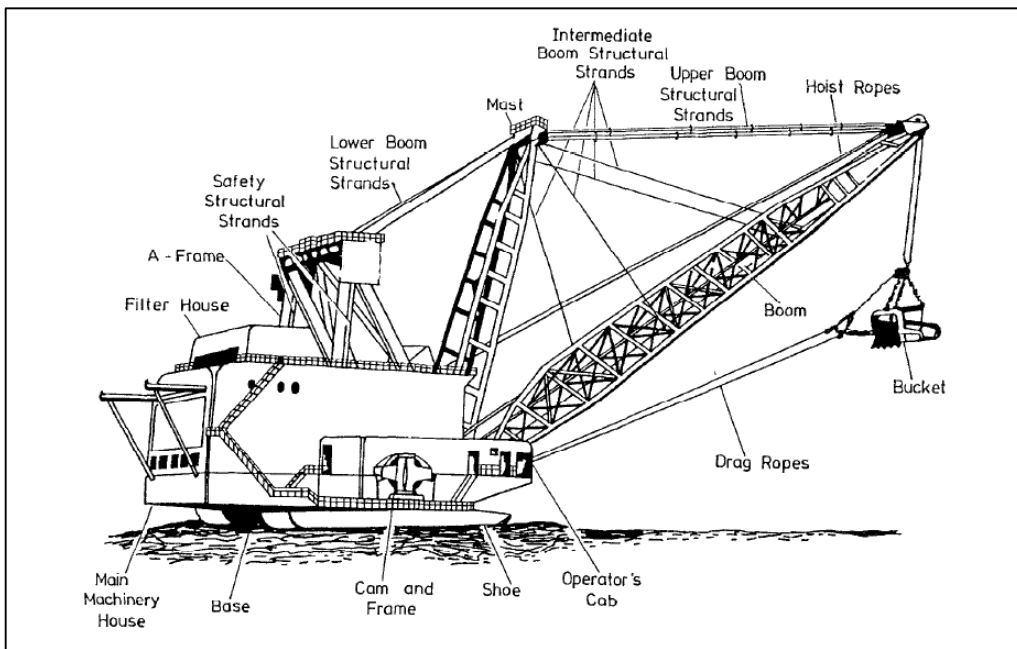


Figure 2.5 Schematic diagrams of dragline components (Mckinnell, 1995)

Dragline working mainly depends on the performance of its front end assembly, which comprises of Boom and gigantic bucket. Construction wise the draglines consist of a lower and upper structure. The upper structure includes operator's cabin, various drives, and excavation and haulage units such as boom, bucket chain, metal ropes and host of assemblies. The lower structure comprises of walking mechanism and metallic chassis along with the rotating structure and tub of the dragline. The tub base of dragline bears a large amount of dragline weight (around 87% of total weight).

2.5 Design of dragline components

There are various components used for design of dragline. The various components of dragline need separate analysis for proper design, to attain maximum life during the operations. On the basis of field observation in Indian coalmines, the main

maintenance and repairing activities are carried out for three main components of dragline. These components are dragline boom along with its associated structure, dragline bucket and suspension ropes. The above mentioned components are required to be monitored regularly during the operation for effective utilization of dragline.

2.5.1 Dragline boom

Dragline booms are constructed using hollow structural steel pipes. They can differ in construction depending on the manufacture and field requirements. It consists of 3 or 4 main chords and 5 or 6 bracing members connected along the length of the dragline. The bracing member form complex overlapping or non-overlapping joints know as boom clusters. These clusters are the complex welded joints which may fail over a certain period of time. Currently in the world there are two types of booms are being used which are Marion dragline boom and BE dragline booms.

2.5.2 Dragline Bucket

In addition to dragline boom, researches about dragline bucket and rigging machine are equally critical, because of the fact that dragline bucket is interacting with the ground. Draglines removes overburden with their massive earth digging buckets, some of which can remove earth greater than 108 m³ (140 yd³) right away (Gilewicz, 1999). Basic construction of bucket with its rigging mechanism has been illustrated in figure 2.6 (Ridley, 2004). Rigging mechanism consist of a hoist chain, dump rope, leave and a drag chain connected with the bucket.

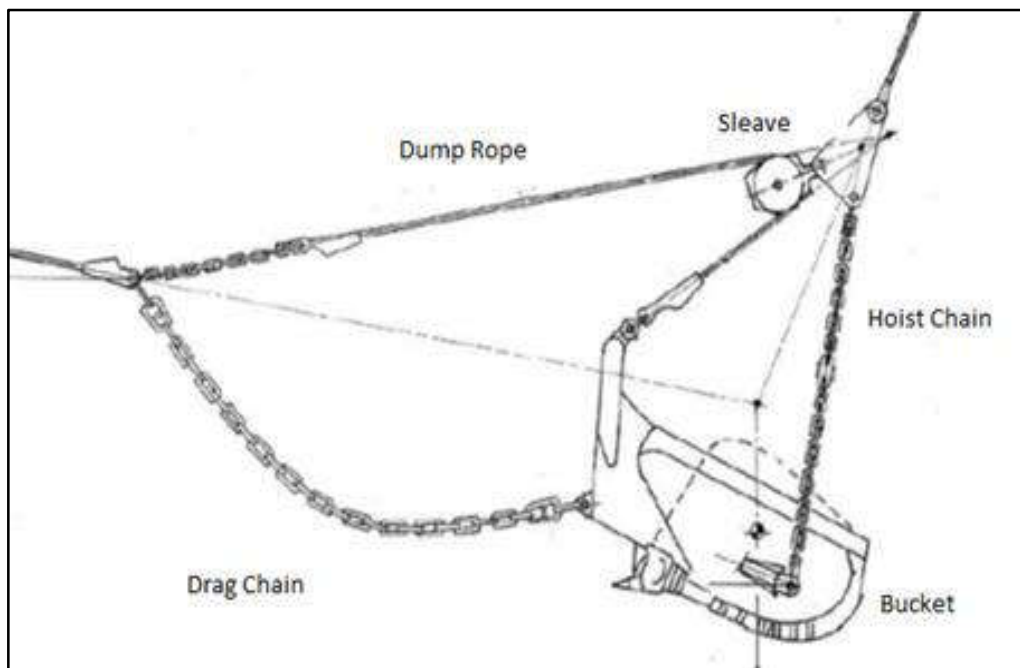


Figure 2.6 Dragline bucket suspension system (Modified after Ridley, 2004)

Design of a dragline bucket includes the dimensional and weight parameters depending on the selection of lip type, shape of the tooth and its number, bucket rigging mechanism, and it affects the overall productivity of dragline operation (Ozdogan, 2003). Therefore, some studies have been carried out to improve the bucket and rigging system of dragline by Ridley and Algra ,2004.

Analytical techniques can be handled as 2D or 3D according to the area of utilization. As cited in Blouin's review study (Blouin et.al, 2001), 3D models (McKyes, 1985; Swick and Perumpral, 1988; Boccafogli et al., 1992) incorporate the effect of accumulated material at the edges of the digging tool during operation. 2D approaches, on the other hand, do not consider the side effect of the formation resistance in modelling (Osman, 1964; Gill and Vanden Berg, 1968; McKyes, 1985; Swick and Perumpral, 1988).

2.5.3 Suspension ropes

There are three types of dragline ropes namely, drag and hoist ropes, IBS and main suspension ropes, and dump ropes, which are different by their functionality. Previous studies on dragline rope maintenance reveal that some of the problems faced by the industries are common to all three categories of ropes while others are more specific to one or more categories.

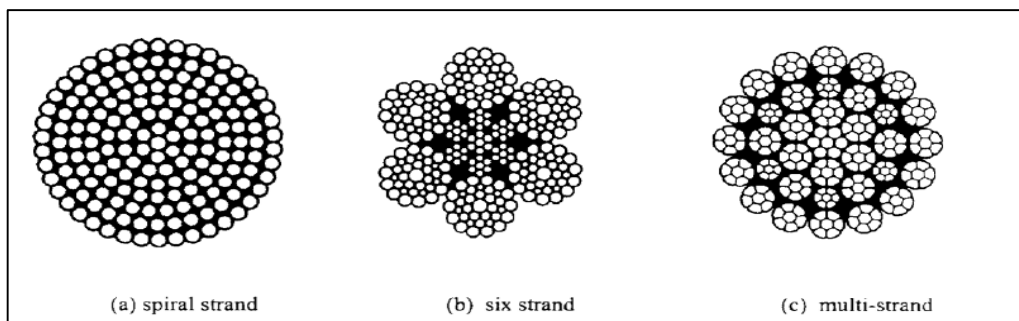


Figure 2.7 Typical rope construction (Chaplin, 2005)

Figure 2.7 shows the typical dragline ropes construction. The ropes used for both hoist and drag are 83 mm in diameter. The recommended (BHP ropes) wire rope construction for hoist ropes is 6×25 FW (12/6 + 6F/1) and 6×49 SF (16/16/8 + 8F/1) for drag ropes. BHP ropes have claimed to have trailed some of their own eight stranded products and monitored the performance of the eight stranded ropes supplied by other manufacturers. However, other studies have shown that the use of eight-strand ropes increases the life of hoist ropes (Golosinski, 1994).

Past researches of the static rope forces under a range of the hoist and drag rope payout lengths using PCDRAG software (Srouf and Shanks, 1995) have shown hoist rope tensions in excess of 200 tonnes (for average bucket payload for dragline), with the bucket positioned well away from the tightline situation, and in excess of 300

Chapter 2: Literature Review

tonnes, when the bucket is positioned near the tight line conditions. It is quite evident that ropes which have high tensile strength are subjected to increased fatigue (Evans and Chaplin, 1997).

The expected service life of drag ropes mainly depends on the condition of the blasted overburden. During digging operations, the drag ropes run through the spoil collecting soil or rock particles on its lubricated surfaces. The soil and rock particles get stuck between individual wires in a strand or between individual strands. The load in the drag ropes can cause the abrasive soil and rock particles to be compressed between two solid surfaces of the individual wires or strands. The high contact pressure produces indentations and scratching of the wearing surfaces and fractures and pulverizes the abrasive ore particles (Hawk and Wilson, 2001)

Sheave and drum size can also have a noteworthy impact on the rope bending fatigue and its operational life. The rope life improvement will be observed as sheave and drum sizes are increased. The rope manufacturers recommend that the sheave and drum sizes are maintained in the range of 25 to 30 times the rope diameters. Reducing the size of drum and sheaves below 25 times rope diameters have a profound effect on rope life (OneSteel, 2001).

Although each component of a dragline is important in its working, but the scope of the current work is limited to design of dragline front end assembly. These components involved dragline A – Frame, mast and dragline boom.

2.6 Dragline Boom Design

The Bucyrus dragline boom consists of a tubular pipe section design with a triangular cross section. The typical boom consists of three (3) main chords running the entire length with lacings connecting the chords to form a lattice type structure. The chord nodes where multiple lacings intersect are identified as “clusters”, the clusters are complex in the way that the lacings connect together and are a critical area for inspection.

The basic design of a boom is shown in figure 2.8. The figure clearly indicates the dragline boom cluster is formed by welding together the main chord with the brace members. The design may differ in terms of overlapping of brace members. Some designs are with overlapping joints and others are with non-overlapping joints.



Figure 2.8 Boom foot and Boom point sheave of a dragline (Dragline Dictionary, 2004)

Boom foot and boom sheave are an integral part of a dragline boom. Boom point sheave consists of a pulley arrangement that connects boom with the bucket during operation by means of hoist ropes. Boom foot is used to erect dragline boom on the site at a particular angle (usually 30 to 40 degrees). It connects the boom lower region with the revolving structure of the dragline.

2.7 Loading of dragline boom

The structural loading on dragline booms is illustrated in Figure 2.9 and depends mainly on the rated suspended load ("RSL") the machine is working at and the capacity of its hoist and swing motors which create the accelerations. Other factors such as the digging pattern, operator characteristics and electrical motor control systems also influence the loading on booms.

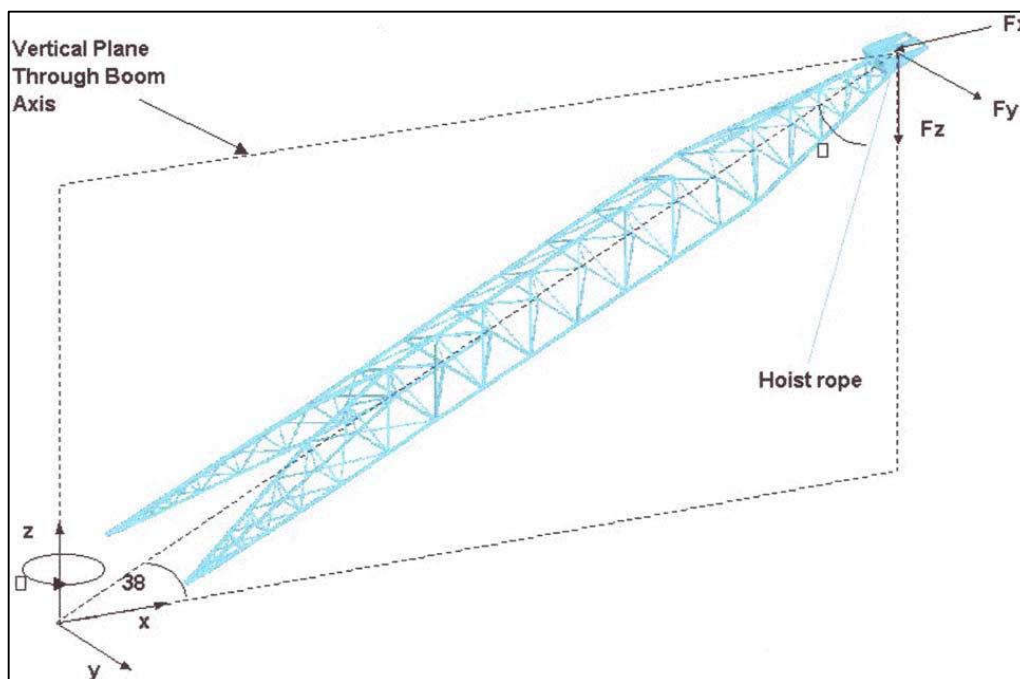


Figure 2.9 The design of a dragline boom with main loadings (Dayawansa et al, 2006)

The main structural components such as booms and masts of BE machines are constructed using tubular structural elements with welded connections which are termed clusters.

The basic load components on dragline boom are as follows

- dead load (i.e. self-weight),
- weight of the bucket acting through the hoist ropes,
- forces from the suspension ropes,
- And the inertia forces mainly due to angular accelerations (dynamic load).

2.8 Design of Joints in boom matrix

General info

Boom is an integral part of a dragline. The design of boom consists of various joints. These joints have been discussed in this section including their failure modes.

2.8.1 The joint according to EUROCODE 3 and CIDECT

Joint is the location in which two or more elements converge. From design prospect, it is a set of basic components (weld seams, bolts, plates, flanges, web, etc.) required to represent the joint behavior on the transmission of appropriate forces throughout the structure (CEN, 2010b). The Chapter 7 of EC 3-1-8, includes detailed application recommendations for the resistance of joints under static loading, with uniplanar or multiplanar geometries, acting upon structures with CHS, RHS or SHS sections (Simões da Silva & Santiago, 2003). In subchapter 7.6 of this document there's the information for the design of joints between hollow and open sections. The IIW and CIDECT recommendations are consistent with each other and they are the root for

the design guide of Wardenier et al (2010). The design of joints between hollow and open sections can be done based on chapter 12 of this design guide. The application rules are valuable for rolled profiles manufactured according to EN 10210-2 (CEN, 2006). The nominal thickness of hollow sections must be between 2.5 and 25 mm, unless special rules are taken to guarantee special properties along the thickness (Simões da Silva & Santiago, 2003).

2.8.2 Type of joints used in lattice structures

Among the different type of joints with hollow sections, in this dissertation it's intended to study the uniplanar joints between hollow and open sections, whereby the open section is the chord and the hollow section is the brace.

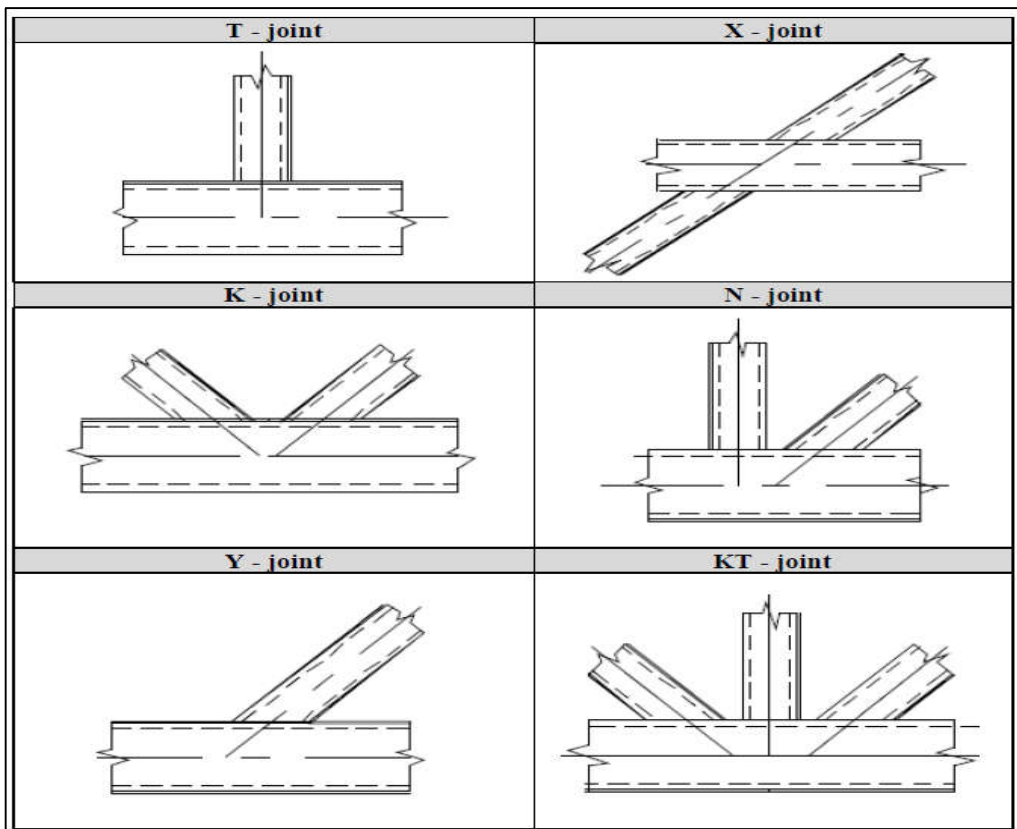


Figure 2.10 Types of joints between hollow and open sections (CEN, 2010b)

The distinct type of uniplanar joints between hollow and open sections can be observed in the figure. It is to note that Y and N joints are similar to T or K joints, but they have difference on the angle between the chord and braces. This difference is taken into account in the resistance formulas, as will be shown afterwards (figure 2.10).

According to Wang et. al., 2013, the classification of the type of joints might vary depending on the load applied to the joints. The classification of joints can also vary depending on the eccentricity of the brace axes in relation to the chord axis and, as already referred, regarding the applied loads.

2.9 Failure Modes of Joints

The different failure modes associated with CHS and RHS joints has been thoroughly discussed in the subsequent section.

2.9.1 Local yield of the brace

The type of failure which corresponds to the local yield of the brace is shown in figure 2.11. As it can be seen from the cutting section A-A in the figure, when the brace is subjected to axial forces, the yield begins in the area of the brace which is closer to the web of I or H profile.

This is an occurrence that happens due to the decreasing of the effective width decrease, explained in the previous subchapter. The Equation (2.6) reflects the resistance of a CHS, RHS or SHS brace when subjected to compression or tension.

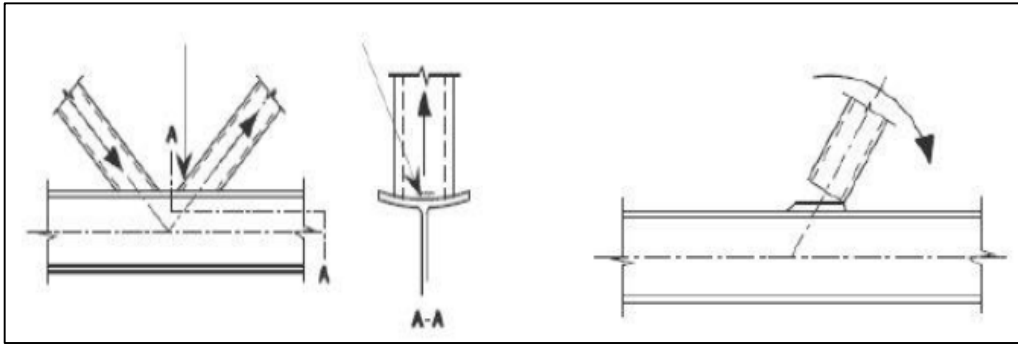


Figure 2.11 Local yields of the brace (CEN, 2010b)

$$N_{1,Rd} = 2\sigma_{yi}t_i b_e \quad (2.6)$$

2.9.2 Chord web failure

The Figure 2.12 shows the type of failure correspondent to the chord web failure.

The Equation (2.7) represents the resistance capacity of the chord web when a CHS, RHS or SHS brace is subjected to a tension or compression force.

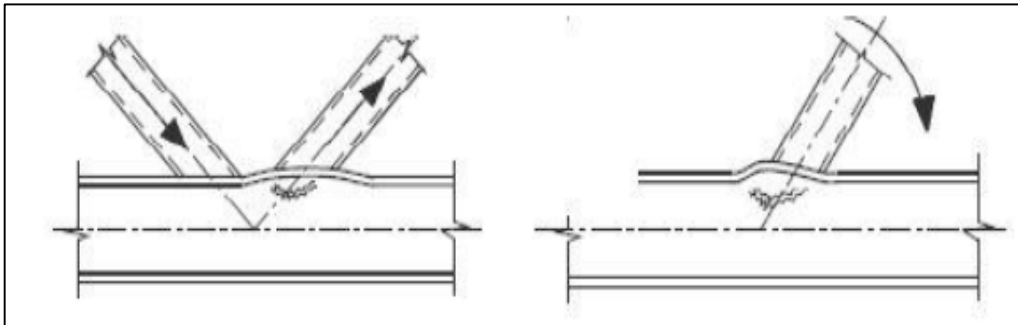


Figure 2.12 Chord web failures (CEN, 2010b)

$$N_{i,Rd} = \frac{2\sigma_{y0}t_w b_w}{\sin \theta_i} \quad (2.7)$$

2.9.3 Chord shear failure

In Figure 2.13 is shown the corresponding type of chord shear failure.

The Equation (2.8) reflects the resistance of a CHS, RHS or SHS brace when subjected to tension or compression forces.

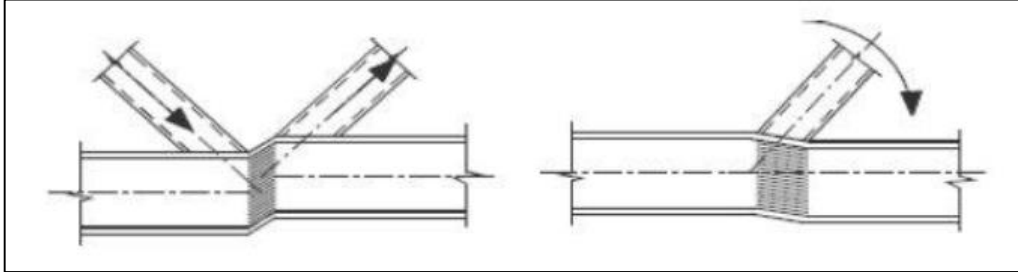


Figure 2.13 Chord shear failure (CEN, 2010b)

$$N_{i,Rd} = \frac{0.58 \sigma_{y0} A_S}{\sin \theta_i} \quad (2.8)$$

The Equation (2.9) reflects the resistance of an I or H chord when subjected to shear forces. According to Simões da Silva & Santiago, (2003), this kind of failure is the most common failure mode in K or N joints with gap between their braces.

$$N_{i,Rd} = (A_0 - A_S) \sigma_{Y0} + A_S \sigma_{y0} \sqrt{1 - \left(\frac{V_{Ed}}{V_{Pl,Rd}} \right)^2} \quad (2.9)$$

2.9.4 Local yielding of overlapping brace

The CIDECT recommendations, in contrast to EC3-1-8, distinguish the effective width equations to be used in overlapped CHS or RHS braces, and consequently the equations are different for this parameter.

The Equation (2.10) represents the resistance of a CHS, RHS or SHS brace when subjected to tension or compression forces and when one of the braces is overlapped by a brace of the same type.

For joints with overlapping braces, the EC 3-1-8 only identifies this failure mode, for different Overlapping percentages. CIDECT identifies more two failure modes (presented soon after) besides this one.

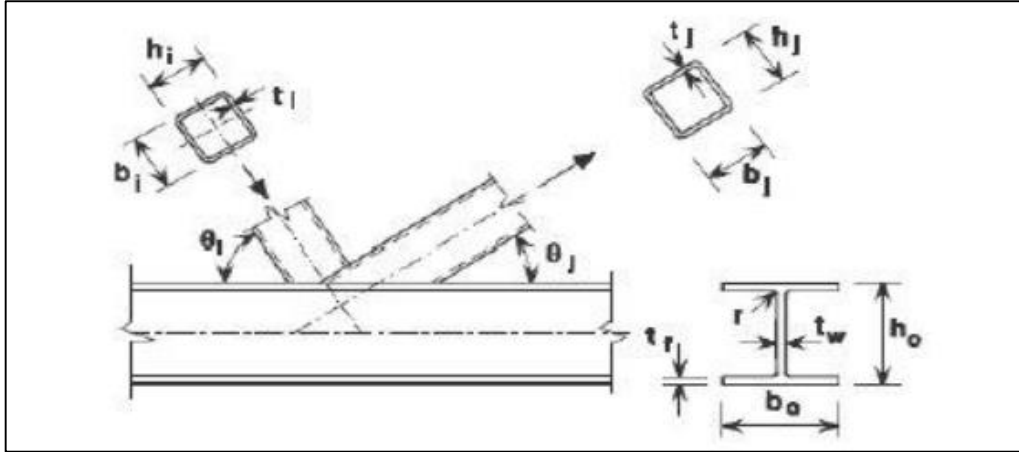


Figure 2.14 Type of joint with overlapping braces (CEN, 2010b)

$$N_{1,Rd} = \sigma_{yi} t_i l_{b.eff} \quad (2.10)$$

2.9.5 Local chord member yielding with overlapping braces

The Equation (2.11) expresses I or H chord resistance when subjected to tension or compression forces combined with bending moment of joints with overlapping braces.

$$\left(\frac{N_0}{N_{pl,0}} \right)^c + \frac{M_0}{M_{pl,0}} \leq 1; C = 1 \text{ For I or H section} \quad (2.11)$$

2.9.6 Brace shear when overlapped by another brace of the same type

The Equation (2.12) consists on the CHS, RHS or SHS brace resistance to shear forces when overlapped by a brace of the same type.

$$N_i \cos \theta_i + N_j \cos \theta_j \leq V_S^* ; O_{V,lim} < O_V < 100\% \quad (2.12)$$

2.9.7 Local yielding of brace when subjected to bending moment

Figure 2.15 presents the referred type of joint subjected to bending moment.

The Equation (2.13) consists on the resistance of a RHS or SHS brace/beam when subjected to bending moment.

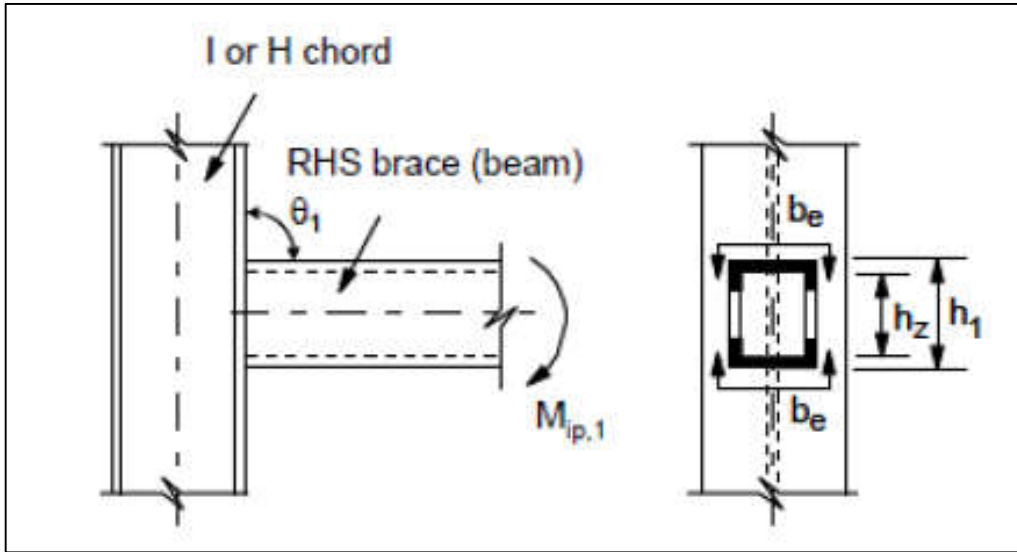


Figure 2.15 T joint subjected to bending moment (CEN, 2010b)

$$M_{ip,1,Rd} = \sigma_{y1} t_1 b_e h_z \tag{2.13}$$

2.9.8 Chord web failure when subjected to bending moment

The Equation (2.14) consists the resistance of a I or H chord/column when subjected to bending moment in a T joint like the one presented in Figure 2.15.

$$M_{ip,1,Rd} = 0.5 \sigma_{yi} t_w b_w (h_1 - t_1) \tag{2.14}$$

The figure 2.16 depict the various failure modes observed in circular hollow sections (CHS) structures as discussed above.

Typical failure modes of CFDST K-joints

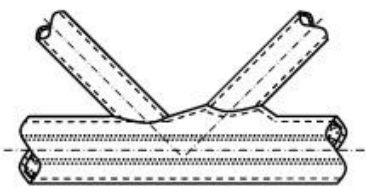
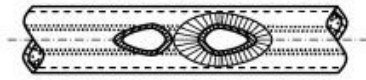
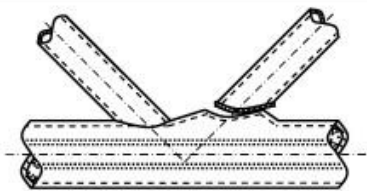
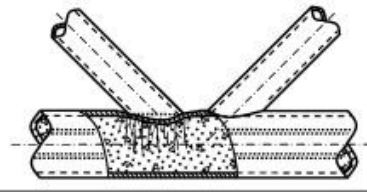
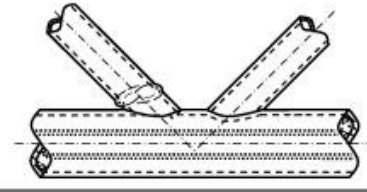
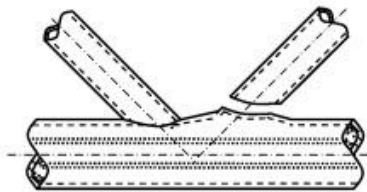
Failure component	Failure mode	Schematic view of failure mode
	Chord plastification	 <p style="text-align: right;">Sectional view</p>
		 <p style="text-align: right;">Top view</p>
Chord failure	Chord punching shear	
	Local bearing failure	
Brace failure	Buckling of the compression brace	
	Fracture of the tension brace	

Figure 2.16 Failure modes for joints between circular hollow sections (Han, 2017)

2.10 Fatigue life

Fatigue life is a mechanical and scientific term that relates to how long an object or material will last before completely failing because of concentrated stresses. ANSYS Fatigue Tool offers two methods to calculate fatigue life. While strain life approach is

Chapter 2: Literature Review

widely used, at present, because of its ability to characterize low cycle fatigue (<100,000 cycles), stress life approach addresses high cycle fatigue (>100,000 cycles).

Engineering fatigue fracture failure is one of the most common phenomena of mechanical and structural failure, statistically representing approximately 50 to 90% of total mechanical damage (Zhao, S.B., Wang, Z.B., 1997). Lattice structures have been widely used in crane booms, steel plants, parking garages, offshore platforms and other fields (Xu, G.N. et.al. 2005).

Generally, the life prediction of elements subjected to fatigue is based on the “safe-life” approach [Sonsino et al.,2012], coupled with the rules of linear cumulative damage (Miner,1945). Indeed, the so-called Palmgren-Miner linear damage rule (LDR) is widely applied owing to its intrinsic simplicity, but it also has some major drawbacks that need to be considered (Schive, 2001), Moreover, some metallic materials exhibit highly nonlinear fatigue damage evolution, which is load dependent and is totally neglected by the linear damage rule (F.H.et al.,2008).The major assumption of the Miner rule is to consider the fatigue limit as material constant, while a number of studies showed its load amplitude-sequence dependence (Xi, L., & Songlin, Z, 2008; Xi, L., & Songlin, Z,2009). Various other theories (Oller et al.,2005; Zalnezhad, E.,2008; Cheng G. X.,1998; Shang D.G.1999; Svensson T.,2002; Jono M.,2005; Makkonen M.,2009; Zhu S.P.and Huang,2010; Grammenoudis et.al.,2009; Rejovitzky, 2013) and models have been developed in order to predict the fatigue life of loaded structures.

2.11 Fatigue life S-N Curve

The American Society for Testing and Materials states that fatigue life, N , of a specimen is the number of stress cycles of a specified manner that a specimen sustains before failure occurs (figure 2.17). Fatigue life is affected by cyclic stresses, residual stresses, material properties, internal defects, grain size, temperature, design geometry, surface quality, oxidation, corrosion, etc. For some materials, notably steel and titanium, there is a theoretical value for stress amplitude below which the material will not fail for any number of cycles, called a fatigue limit, endurance limit, or fatigue strength.

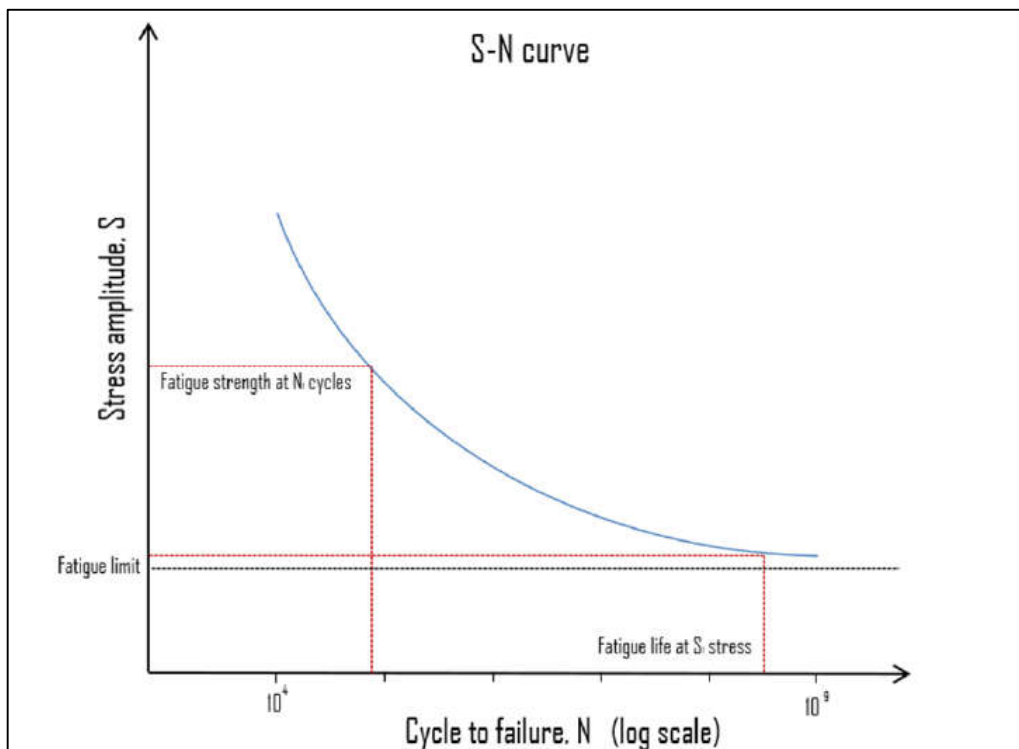


Figure 2.17 S-N curve for a material (William and David, 2003)

2.12 Failure analysis criteria

A range of theoretical standards were proposed for acquiring better correlation between envisioned factor in existence and that achieved underneath carrier load conditions for both brittle and ductile materials. The five main theories are:

- a. Maximum principal stress theory (Rankine).
- b. Maximum shear stress theory (Guest-Tresca).
- c. Maximum principal strain (Saint-Venant).
- d. Total strain energy per unit volume (Haigh).
- e. Distortion energy theory (Von Mises yield criterion).

In the present study, the distortion energy theory (Von Mises yield criterion) has been used for analysis. According to this theory, yielding would occur when total distortion energy absorbed per unit volume due to applied loads exceeds the distortion energy absorbed per unit volume at the tensile yield point (Hearn, 1997).

Total strain energy E_T and strain energy for volume change E_V can be given as:

$$E_T = \frac{1}{2} (\sigma_1 \epsilon_1 + \sigma_2 \epsilon_2 + \sigma_3 \epsilon_3) \quad (2.15)$$

$$E_V = \frac{3}{2} \sigma_{av} \epsilon_{av} \quad (2.16)$$

Substituting strains in terms of stresses the distortion energy can be given as

$$E_d = E_T - E_V = \frac{2(1 + \nu)}{6E} (\sigma_1^2 + \sigma_2^2 + \sigma_3^2 - \sigma_1 \sigma_2 - \sigma_2 \sigma_3 - \sigma_3 \sigma_1) \quad (2.17)$$

At the tensile yield point, $\sigma_1 = \sigma_y$, $\sigma_2 = \sigma_3 = 0$ which gives,

$$E_{dy} = \frac{2(1 + \nu)}{6E} \sigma_y^2 \quad (2.18)$$

The failure criterion is thus obtained by equating E_d and E_{dy} , which gives,

$$(\sigma_1 - \sigma_2)^2 + (\sigma_2 - \sigma_3)^2 + (\sigma_3 - \sigma_1)^2 = 2\sigma_y^2 \quad (2.19)$$

In a 2-D situation if $\sigma_3 = 0$, then

$$\sigma_1^2 + \sigma_2^2 - \sigma_1\sigma_2 = \sigma_y^2 \quad (2.20)$$

i.e.

$$\left(\frac{\sigma_1}{\sigma_y}\right)^2 + \left(\frac{\sigma_2}{\sigma_y}\right)^2 - \left(\frac{\sigma_1}{\sigma_y}\right)\left(\frac{\sigma_2}{\sigma_y}\right) = 1 \quad (2.21)$$

This is an equation of the ellipse, and the yield surface is shown in Figure 2.18. This theory is accepted to be valid for ductile materials. However, this theory has the following limitations.

- The theory does not apply to brittle materials for which the elastic limit stress in tension and compression is quite different.
- It cannot be applied for materials under hydrostatic pressure.

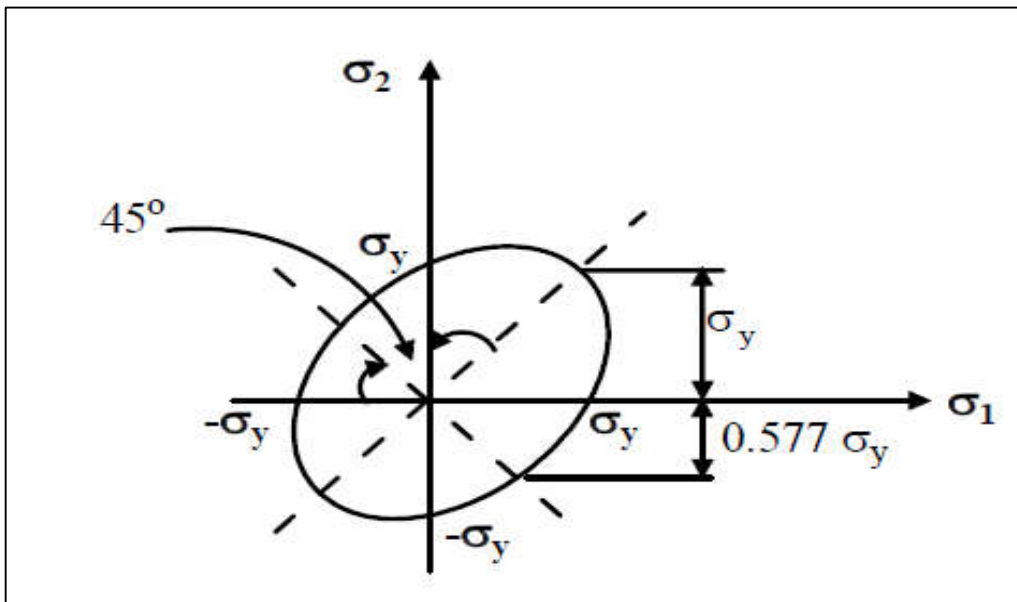


Figure 2.18 Yield surface corresponding to the Von Mises yield criterion (Hearn, 1997)

The value of stress for a particular material used for a specific way, which is considered to be safe stress, is usually called the working stress. For static applications, the working stress of ductile materials is usually based on yield strength. The working stress may be considered as either the yield strength or the tensile strength divided by a number called the factor of safety. If failure would result in loss of life, the factor of safety should be increased.

$$\text{Factor of safety (N)} = \text{yield strength/working stress}$$

2.13 Finite element analysis

In Turner et al. (1956), the application of finite elements has been presented for the analysis of aircraft structures and it is referred to as one of the key contributions in the development of the FEM. It is rightly addressed in Hutton (2004) that FEM is a computational technique used to obtain approximate solutions of boundary value problems in engineering. As a result, the FEM has been implemented rigorously for solving a wide variety of problems in applied science and engineering and it has been rapidly developed over the years (Rao, 2004).

One of the recent trends in solving the above mentioned problems is specifically based on FEM and its research development is reviewed in this domain. As regards these issues, in Öz (2000) natural frequencies of an Euler–Bernoulli beam-mass system are calculated using this approach. Two finite element formulations of Reddy’s higher-order theory, assuming different values for C_0 , were used in Nayak et al. (2002) to obtain the natural frequencies of composite and sandwich plates. In Chakraborty et al. (2003) a new beam finite element has been proposed based on the

first-order shear deformation theory to study the thermo-elastic behavior of functionally graded (FG) beam structures.

2.13.1 Basic idea of finite element analysis

Finite element analysis (FEA) has been used for analysis and simulation under different loading conditions of the excavator components. The FEM analysis of any structural element supports in forecasting the structural masses and design in which it will act under stressed conditions (Azam & Rai, 2018). Finite Element Analysis (FEA) is a computational simulation approach imparting one-of-a-kind possibilities to analyse physical conditions such as displacement, stress and strain, force, velocity, and acceleration, mass on stable bodies by the use of a numerical identity known as a finite element. FEA drives complicated configurations of factors named as a node. It generates adjacent grids named as mesh, the usage of the nodes. The mesh has a network formation where each adjacent node is connected. This mesh network involves material and structural specifications to identify how the structure will respond to different analysis conditions. As an example, to FEA utility, a blade cutting operation is illustrated in Figure 2.19. Structural analysis in FEA carries linear and nonlinear models. Linear functions make use of simple parameters and assume that the deformation of a material isn't plastic. On the alternative hand, nonlinear functions can examine the stress on the fabric while the elastic functionality of it is surpassed. Therefore, stress values in nonlinear functions keep changing with plastic deformation.

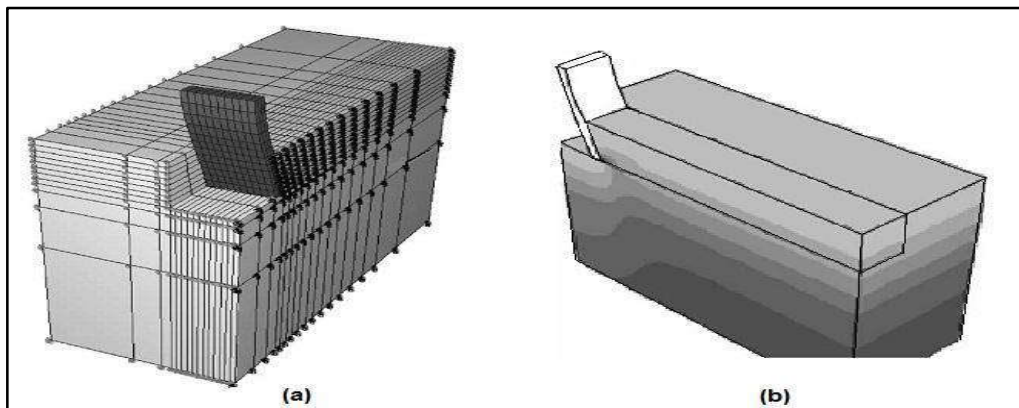


Figure 2.19 FEA (a) Meshing (b) Stress Distribution (Abo-Elnor et al. 2004)

2.13.2 Applications of finite element analysis in earthmoving equipment

An earthmoving action expresses the shape of interaction between the formation and the digging tool. This interaction is mainly affected by formation specifications such as density, internal friction angle, external friction angle, cohesion and adhesion.

Earthmoving elements shape an entirely complicated phenomenon. The formation can exhibit either isotropic or anisotropic nature. If it is anisotropic, formation specifications change mainly with the direction of forces inside the formation, and it is hard to estimate such behavior. Moreover, compactness of the formation can entirely change the influence on the digging tool. All dynamics of the formation are required to be known to see the full interaction between tool and formation. However, it is hard to identify the full effect of the formation on the tool. Under these conditions, it is better to characterize the tool-formation interaction in reality, with some assumptions.

Many investigators have used FEA to address troubles related to earthmoving movements. Yong and Hanna (1977) worked on the productivity of a flat blade moving in clay formation for a distance smaller than one foot. It was claimed that

Chapter 2: Literature Review

they proposed a method that gave a unique value of the stress and deformation of the formation due to the excavation forces. It was stated that the method provided advantage in the estimation of forces exerted by both the tool and the formation.

Mouazen and Nemenyi (1999) created an elastic-perfectly plastic formation model and used FEA to simulate the formation cutting process of a sub formation for varying geometries. Fielke (1999) performed a computational model expressing the effect of cutting-edge geometry over the tillage forces. The experimental results supported this two-dimensional finite element model. Mootaz et al. (2003) performed the three-dimensional simulation of narrow blade-formation interaction in an FEA solver, by assuming that formation behaves elastically. They tested formation failure zones vertically and horizontally to eliminate convergence trouble precipitated due to large blade movement. The model was validated by providing the ultimate shear stress zones in the formation after computing the software and matching it with the predefined formation failure areas. In a two-dimensional approach, Davoudi et al. (2008) insisted that a model which is capable of estimating draft forces during tillage was created in FEA software. Moreover, in many research, brittle behavior and plasticity of formation during the cutting process was analyzed (Chi and Kushwaha, 1989; Raper and Erbach, 1990; Aluko and Chandler, 2004; Aluko, 2008).

Besides FEA, the reader can decide on to use DEM for the tool-formation interaction modelling, although it is mainly deployed for the simulation of granular materials and for analysing the connection among inter-particle and particle-tool behaviours (Cleary, 1998; Owen et al., 2002; Hofstetter, 2002).

2.14 Summary of the literature review

Literature survey describes the previous researches in respect of dragline earthmoving operation and theories at the back of this phenomenon. These researches organised a historical past for the thesis challenge, research of stresses on the dragline boom with FEA. The literature seeks started with the general data about dragline usage on the sector open-cast mines and dragline stripping methods. Then, it proceeds with the method of the selection of dragline with its required bucket capacity, boom angle and boom length etc.

After a peer review of dragline and productiveness, literature seeks advancement in a more significant specific subject. In this element, it turned into tried to create a basis for dragline boom simulation. To attain this, components of finite element evaluation, concepts of earthmoving operations and factors affecting the stresses in the joints of boom were analysed.

From the literature survey, it is clearly evident that there exists a gap in the areas of stress investigation of the dragline boom and the analysis of the stresses. Therefore, the thesis aims to contribute to the knowledge, with three-dimensional dragline boom simulation, stress value investigation and effect of different parameters on the stress values of the boom.